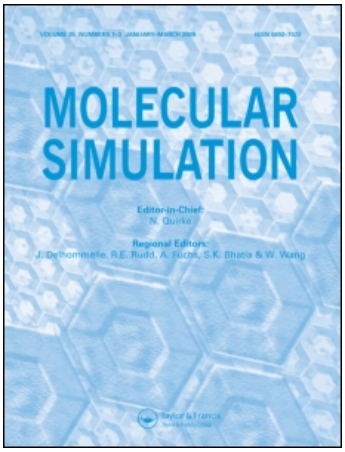

Molecular Simulation
Publication details, including instructions for authors and subscription information:
http://www.informaworld.com/smpp/title~content=t713644482

Depletion interaction in colloid/polymer mixtures: application of density functional theory

X. Chen[a]; J. Cai[a]; H. Liu[a]; Y. Hu[a]
[a] State Key Laboratory of Chemical Engineering and Department of Chemistry, East China University of Science and Technology, Shanghai, People's Republic of China

To cite this Article Chen, X. , Cai, J. , Liu, H. and Hu, Y.(2006) 'Depletion interaction in colloid/polymer mixtures: application of density functional theory', Molecular Simulation, 32: 10, 877 — 885
To link to this Article: DOI: 10.1080/08927020600935580
URL: http://dx.doi.org/10.1080/08927020600935580

Molecular Simulation, Vol. 32, Nos. 10–11, 30 August–15 September 2006, 877–885

Taylor & Francis
Taylor & Francis Group

Depletion interaction in colloid/polymer mixtures: application of density functional theory

X. CHEN, J. CAI, H. LIU* and Y. HU

State Key Laboratory of Chemical Engineering and Department of Chemistry, East China University of Science and Technology, Shanghai 200237, People's Republic of China

(Received June 2006; in final form July 2006)

Insert-route density functional approach (IRDFT), modified fundamental measure theory (MFMT) and thermodynamic perturbation theory (TPT1 and TPT2) are combined to study the depletion force between colloidal particles in hard sphere/hard sphere chain mixtures which represent a model of systems containing colloids dispersed in an athermal polymer solution. The predicted results are compared to simulations showing the reliability of the method used which captures the main characteristics of depletion interaction between colloids induced by polymers. Results of TPT2 are slightly more repulsive and better than that of TPT1 especially when the inter-particle distance is small than the diameter of polymer segment indicating the essential influence of the three-body correlations. Effects of the polymer density, polymer chain length and size ratio of colloid to polymer segment on the depletion force are studied in detail. Due to a little deterioration of the prediction in the high density region, further improvement is anticipated to better balance the competition between the excluded-volume effect and the chain connectivity.

Keywords: Depletion interaction; Colloid/polymer mixtures; Modified fundamental measure theory; Thermodynamic perturbation theory

1. Introduction

Behavior of colloidal particles in polymeric systems has attracted sustained experimental and theoretical efforts because of its relevance to colloidal stability, also to the preparation of composite materials, proteins in living cells, where the colloidal stability plays important role. Two categories can be distinguished. The polymer molecules attached on the colloidal particle surface by grafting or adsorption, protect the colloids from flocculation; it is usually called steric stabilization. The free polymer molecules also have important effect on colloid stability; it is correspondingly called depletion stabilization or depletion flocculation. This work primarily deals with the latter. The key to the understanding of the behavior of such depletion systems is the effective interaction potential between the colloid particles, which is a sum of the direct intercolloidal potential and the depletion potential. A basic model of such systems is a mixture of big hard spheres and freely jointed hard sphere chains served as depletant, which was first studied by Asakura and Oosawa [1]. The mixture corresponds to hard colloidal particles dispersed in an athermal polymer solution. For these hard colloidal particles, the effective interaction is mainly determined by depletion force induced by the depletant.

In recent years, different methods have been developed for the estimation of depletion force in hard sphere mixtures, among them, the most fruitful are computer simulation [2,3], integral equation theory (IET) [3] and density functional theory (DFT) [4–7]. Attard [8] firstly derived an exact expression for the depletion force in terms of the equilibrium density profile of fluid from the DFT. The crux of applying this formula to calculate depletion force is the requirement of density distribution of small-spheres (depletant) around two fixed big spheres (colloids). However, although one could get the two-dimensional density profile (which has the axial symmetry and depends on two parameters) directly through molecular simulation [2,3], it is rather time consuming. Various efforts have turned to theoretical calculations. Naturally, Kirkwood superposition approximation (KSA) [9] can be employed to simplify the calculation if only the one-dimensional profile (which is obtained by fixing a single colloid so that the profile has radial symmetry and depends only on the distance r from the center) is involved

*Corresponding author. Email: hlliu@ecust.edu.cn

Molecular Simulation
ISSN 0892-7022 print/ISSN 1029-0435 online © 2006 Taylor & Francis
http://www.tandf.co.uk/journals
DOI: 10.1080/08927020600935580

[2,8]. The more strict approach with Attard's formula is to calculate the two-dimensional profile but with higher computational costs [5–7]; the method is usually called the brute-force DFT (BFDFT).

In fact, as it has been adopted in the long-standing primitive model in the field of electrolytes, a binary mixture could be mapped onto an effective one-component system by a procedure originally developed by McMillan and Mayer [10], whereby a statistical mechanical definition of depletion potential is obtained [11]. Based on this definition, Roth *et al.* [4] derived depletion potential by just using the density distribution around one single colloid particle that circumvents the superposition approximation by combination of the potential distribution theorem [12] and the DFT equation of mixture; it is called the insert-route density functional approach (IRDFT). Compared with the above BFDFT method, this IRDFT method avoids the complication of numerical calculation and limitations that are inherent in BFDFT. The accuracy of BFDFT determined by the well calculation of density distribution around two colloids is now realized by finding a good approximation to the Helmholtz energy functional of the mixture in the external field of one fixed colloid particle by IRDFT. Given a perfect density functional of mixture, IRDFT in the dilute limit (i.e. the density of colloids going to zero) is equivalent to BFDFT [13].

On the colloid/polymer mixtures, studying the depletion force theoretically has attracted growing attention. Very recently, Patel and Egorov [14] calculated the effective interaction between two hard particles in athermal polymer solutions by BFDFT indicating the invalidity of KSA in polymer solutions. Hopper *et al.* [15] utilized polymer reference interaction site model (PRISM) IET to discuss the depletion of two particles in a dense polymer solution or melt. Sulve *et al.* [16] studied the depletion interactions of proteins in polymer solutions by self-consistent field theory (SCFT). Kim and Lee [17] developed the IRDFT for colloid–polymer mixtures based on the weighted-density approximation (WDA) by using a simple weighting function to investigate the depletion effects for two colloids and provided good results.

In this work, we adopt IRDFT to study the depletion force in colloid/polymer system where a binary mixture of hard sphere and flexible hard sphere chain is involved. Unlike the IRDFT for hard sphere mixtures, the connectivity between monomers characterizing the chain polymers should be considered in the density profile as the input of IRDFT and in the functional of IRDFT itself as well. The DFT we employed gives more information about the correlation between the monomers than that in SCFT and avoids the trouble of finding an appropriate closure-relation in PRISM IET. The Rosenfeld's fundamental measure theory (FMT) [18] modified by Yu and Wu [19] (see also Roth *et al.* [20]), is adopted in the DFT approach to define the weighting functions. Thermodynamic perturbation theory of Wertheim [21] that includes the two versions of TPT1 and TPT2, is also employed in building the model.

The remainder of the paper is organized as follows. In Section II, we outline the models and methods employed. In Section III, we compare our theoretical results with computer simulations and discuss the effects of input density profiles and modification of present functional. Finally, we summarize the conclusion in Section IV.

2. Theory and method

2.1 IRDFT for colloid/polymer systems

IRDFT developed by Roth *et al.* [4] is based on the potential distribution theorem [12] which is a general result, valid for arbitrary number of components and arbitrary inter-particle potential functions. In principle, it can be applied for the colloid/polymer systems. We first fix a colloid particle at the origin. Then insert the second test colloid particle at position **r** from the origin. Because of the symmetry, the depletion potential depends only on the scalar *r*. IRDFT gives directly the depletion potential $V_c^{dep}(r)$ and the depletion force $f_c^{dep}(r)$ in terms of the one-body direct correlation function $c_c^{(1)}(r)$ by the following equations, here the subscript c denotes colloid,

$$\beta V_c^{dep}(r) = c_c^{(1)}(r \to \infty; [\rho_c \to 0, \rho_p]) - c_c^{(1)}(r; [\rho_c \to 0, \rho_p]) \tag{1}$$

$$\beta f_c^{dep}(r) = -\frac{d\beta V_c^{dep}(r)}{dr} \tag{2}$$

The merit of the IRDFT lies in the fact that the direct correlation function in the above equations depends on the equilibrium density profile before the second test colloid particle is inserted at position **r**. This measure greatly simplifies the calculations compared with the BFDFT. To obtain the direct correlation function, we need density profiles. Therefore, we need to establish a suitable DFT model for the colloid/polymer systems.

2.2 DFT model for colloid/polymer systems

We model the colloids as hard spheres of diameter σ_c and the polymers as chains composed of *M* tangentially bonded hard sphere segments of diameter σ_{ps}, here the subscript ps denotes polymer segment. Within the DFT approach, the grand potential of the system, Ω is a functional of the local densities of polymers and colloids, $\rho_p(\mathbf{R})$ and $\rho_c(\mathbf{r})$, respectively, the subscript p denotes polymer,

$$\Omega[\rho_p(\mathbf{R}), \rho_c(\mathbf{r})] = F[\rho_p(\mathbf{R}), \rho_c(\mathbf{r})] + \int d\mathbf{R}\rho_p(\mathbf{R})\left[V_p^{ext}(\mathbf{R}) - \mu_p\right] + \int d\mathbf{r}\rho_c(\mathbf{r})\left[V_c^{ext}(\mathbf{r}) - \mu_c\right] \tag{3}$$

where $V_{\rm p}^{\rm ext}(\mathbf{R}) = \sum_{i=1}^{M} \varphi_{\rm p}^{\rm ext}(\mathbf{r}), V_{\rm c}^{\rm ext}(\mathbf{r})$, $\mu_{\rm p}$ and $\mu_{\rm c}$ are the external potentials and the chemical potentials for polymers and colloids, respectively. $\mathbf{R} = \{\mathbf{r}_1, \mathbf{r}_2, \ldots, \mathbf{r}_M\}$, denotes a set of monomer coordinates. The free energy functional F of the system is a sum of the ideal and excess contributions, $F = F^{\rm id} + F^{\rm ex}$. The ideal part of the free energy functional is known exactly as

$$\begin{aligned}\beta F^{\rm id}[\rho_{\rm p}(\mathbf{R}), \rho_{\rm c}(\mathbf{r})] =& \beta \int {\rm d}\mathbf{R} \rho_{\rm p}(\mathbf{R}) V_{\rm b}(\mathbf{R}) \\ &+ \int {\rm d}\mathbf{R} \rho_{\rm p}(\mathbf{R}) \left[\ln\left(\Lambda_{\rm p}^3 \rho_{\rm p}(\mathbf{R})\right) - 1\right] \\ &+ \int {\rm d}\mathbf{r} \rho_{\rm c}(\mathbf{r}) \left[\ln\left(\Lambda_{\rm c}^3 \rho_{\rm c}(\mathbf{r})\right) - 1\right] \end{aligned} \quad (4)$$

Where the total bonding potential for a polymer chain $V_{\rm b}(\mathbf{R})$, is represented as a sum of the bonding potentials $\upsilon_{\rm b}$ between the monomers,

$$\begin{aligned} V_{\rm b}(\mathbf{R}) &= \sum_{i=1}^{M} \upsilon_b(|r_{i+1} - r_i|), \\ \exp[-\beta V_{\rm b}(\mathbf{R})] &= \prod_{i=1}^{M} \frac{\delta(|\mathbf{r}_{i+1} - \mathbf{r}| - \sigma_{\rm ps})}{4\pi\sigma_{\rm ps}^2} \end{aligned} \quad (5)$$

The excess free energy $\beta F^{\rm ex}\{\rho_{\rm ps}(\mathbf{r}), \rho_{\rm c}(\mathbf{r})\}$ is expressed as a functional of the local density of colloids $\rho_{\rm c}(\mathbf{r})$ and the average segment local density $\rho_{\rm ps}(\mathbf{r})$ defined as

$$\rho_{\rm ps}(\mathbf{r}) = \sum_{i=1}^{M} \rho_{{\rm ps},i}(\mathbf{r}) = \sum_{i=1}^{M} \int {\rm d}\mathbf{R}\, \delta(\mathbf{r} - \mathbf{r}_i) \rho_{\rm p}(\mathbf{R}) \quad (6)$$

To estimate the excess free energy functional, the FMT formalism of Rosenfeld [18] is adopted. The excess free energy functional is expressed as [22]

$$\beta F^{\rm ex}[\rho_{\rm ps}(\mathbf{r}), \rho_{\rm c}(\mathbf{r})] = \int {\rm d}\mathbf{r} \left[\Phi_{\rm hs}(\{n_\alpha(\mathbf{r})\}) + \Phi_{\rm chain}(\{n_\alpha(\mathbf{r})\})\right] \quad (7)$$

Where $\Phi_{\rm hs}(\{n_\alpha(\mathbf{r})\})$ and $\Phi_{\rm chain}(\{n_\alpha(\mathbf{r})\})$ are the reduced excess free energy density functional relevant to the hard sphere contribution as a reference and the chain connectivity contribution as a perturbation, respectively. Altogether six $n_\alpha(\mathbf{r})$ with $\alpha = 0$, 1, 2, 3 and $\alpha = V1$, $V2$ are scalar and vector weighted densities, defined as

$$n_\alpha(\mathbf{r}) = \sum_{i={\rm ps,c}} n_\alpha^{\rm i}(\mathbf{r}) = \sum_{i={\rm ps,c}} \int {\rm d}\mathbf{r}' \rho_i(\mathbf{r}') w_\alpha^i(\mathbf{r} - \mathbf{r}') \quad (8)$$

Where the subscript of the summation, j counts in both the polymer segments and the colloids. Six w_α are the weighting functions corresponding to the six weighted densities. The functional $\Phi_{\rm hs}(\{n_\alpha(\mathbf{r})\})$ is evaluated using the "White bear" version [19,20] of FMT. Details of the expressions of $\Phi_{\rm hs}(\{n_\alpha(\mathbf{r})\})$ and the weighting functions are listed in Appendix.

The equilibrium density profiles of polymers and colloids could be found from the condition,

$$\frac{\delta\Omega}{\delta\rho_{\rm p}(\mathbf{R})} = \frac{\delta\Omega}{\delta\rho_{\rm c}(\mathbf{r})} = 0 \quad (9)$$

The one-body direct correlation function is calculated by

$$\begin{aligned} c_{\rm c}^{(1)}(\mathbf{r}) &= -\frac{\delta\beta F^{\rm ex}[\rho_{\rm ps}(\mathbf{r}), \rho_{\rm c}(\mathbf{r})]}{\delta\rho_{\rm c}(\mathbf{r})} \\ &= \beta\left[V_{\rm c}^{\rm ext}(\mathbf{r}) - \mu_{\rm c}\right] + \ln\Lambda_{\rm c}^3 \rho_{\rm c}(\mathbf{r}) \end{aligned} \quad (10)$$

In the above equations, the functional $\Phi_{\rm chain}(\{n_\alpha(\mathbf{r})\})$ is remained to be further discussed.

2.3 The reduced excess free energy density functional relevant to the chain connectivity

We adopt Wertheim's first-order and second-order TPT1 and TPT2 [20].

2.3.1 TPT1. Yu and Wu's formulation [22] is adopted to calculate $\Phi_{\rm chain}^{\rm TPT\,1}$. The details are listed in the Appendix.

2.3.2 TPT2. TPT2 considers the three-body correlations that are neglected in TPT2. For a bulk fluid, the TPT2 reduced excess energy density due to chain connectivity is given by

$$\begin{aligned} \Phi_{\rm chain}^{\rm TPT2} = \Phi_{\rm chain}^{\rm TPT1} + \frac{\rho_{\rm ps}}{M} \ln\sqrt{1+4\omega} \\ \times \left[\left(\frac{\left(1+\sqrt{1+4\omega}\right)}{2}\right)^M - \left(\frac{\left(1-\sqrt{1+4\omega}\right)}{2}\right)^M\right] \end{aligned} \quad (11)$$

where ω concerns with the three-body correlation function evaluated by the expression based on simulation of Müllar and Gubbins [23],

$$\omega = 0.233633\eta_{\rm ps}(1 + 0.472\eta_{\rm ps}) \quad (12)$$

Here, $\eta_{\rm ps} = \pi\sigma_{\rm ps}^3\rho_{\rm ps}/6$ is the reduced density of the polymer segments.

For inhomogeneous systems, similar to the treatment on $\Phi_{\rm chain}^{\rm TPT\,1}$ by Yu and Wu [22], $\rho_{\rm ps}$ and $\eta_{\rm ps}$ are replaced by the weighted densities $n_0^{\rm ps}\zeta_{\rm ps}$ and $n_3^{\rm ps}$ defined by FMT.

2.4 Numerical method

The equilibrium density profile of hard chain polymer is needed as input. It is obtained as usual by

$$\rho_{\rm ps}(\mathbf{r}) = \exp\{\beta[\mu_{\rm p} - \lambda(r)]\} \sum_{i=1}^{M} G_i(r) G_{M+1-i}(r) \quad (13)$$

Where the effective external potential $\lambda(r)$ and propagator function $G_i(r)$ are determined by

$$\lambda(r) = \frac{\delta F^{\rm ex}}{\delta\rho_{\rm ps}(\mathbf{r})} + \varphi_{\rm p}^{\rm ext}(r), \quad (14)$$

$$\begin{aligned} G_i(r) = &\int {\rm d}r' \exp[-\beta\lambda(r)] \\ &\times \frac{r'\Theta(\sigma_{\rm ps} - |\mathbf{r} - \mathbf{r}'|)}{2\sigma_{\rm ps} r} G_{i-1}(r') \end{aligned} \quad (15)$$

where $G_1 = 1$, $i = 2, \ldots, M$.

2.5 KSA method for colloid/polymer systems

In order to calculate depletion interaction and compare with the results of KSA, a dilute limit in which the density of colloids approaches zero is considered here. Equations (1) and (2) only needs the average segment density as an input. In the KSA approach, only the one-dimensional density profile is needed also. The corresponding result for the depletion force reads

$$\beta f_{\mathrm{KSA}}(r) = \frac{\pi\rho_{\mathrm{c}}(\sigma_{\mathrm{pc}})}{r^2\rho_{\mathrm{ps}}^{\mathrm{bulk}}}\int_{r+\sigma_{\mathrm{pc}}}^{\sqrt{r^2+\sigma_{\mathrm{pc}}^2-2r\sigma_{\mathrm{pc}}\cos\theta_{\min}}} \times \mathrm{d}r'\, r'\left(r^2+\sigma_{\mathrm{pc}}^2-r'^2\right)\rho_{\mathrm{ps}}(r') \qquad (16)$$

Where

$$\sigma_{\mathrm{pc}} = \frac{\sigma_{\mathrm{ps}}+\sigma_{\mathrm{c}}}{2},$$

$$\cos\theta_{\min} = \begin{cases} 1+\frac{r-2\sigma_{\mathrm{pc}}}{2\sigma_{\mathrm{pc}}\sigma_{\mathrm{ps}}} & r < 2\sigma_{\mathrm{pc}} \\ 1 & r \geq 2\sigma_{\mathrm{pc}} \end{cases} \qquad (17)$$

3. Results and discussions

3.1 Compare predicted results with simulations and with that by KSA

To test the theoretical results, we adopt simulation data by Striolo *et al.* [24]. We select three sets of parameters employed in the MC simulations as follows: $\sigma_{\mathrm{ps}}^3\rho_{\mathrm{ps}}^{\mathrm{bulk}} = 0.1$, $M = 30$; $\sigma_{\mathrm{ps}}^3\rho_{\mathrm{ps}}^{\mathrm{bulk}} = 0.225$, $M = 20$; and $\sigma_{\mathrm{ps}}^3\rho_{\mathrm{ps}}^{\mathrm{bulk}} = 0.3$, $M = 10$. In all three cases, the colloid diameter is five fold as large as that of the polymer segment, $\sigma_{\mathrm{c}} = 5\sigma_{\mathrm{ps}}$. The input density profile for IRDFT and KSA approach is calculated from DFT and TPT1. When $M = 1$, the hard sphere chain reduces to hard sphere. Figure 1 shows the dependence of the depletion force between colloid particles in hard sphere mixtures on the inter-particle distance calculated by KSA and IRDFT. Since the IRDFT results were compared to simulations and agree very well [4] and the KSA results are so close to the IRDFT results, one can conclude that also the KSA results agree well with simulations. When $M > 1$, for colloid/polymer systems, as shown in figure 2, although the depletion force given by KSA method is good when the inter-particle distance is large, the accuracy gradually deteriorate when the two colloidal particles are getting closer. The prediction by IRDFT is much better in comparison with the simulation especially in the short inter-particle distance range showing the reliability of the method used which captures the main characteristics of depletion interaction between colloids induced by polymers. A comparison with figures 1 and 2 implies a fact that the chain connectivity makes the force more repulsive at small intercolloidal separation and more attractive at large intercolloidal separation in a polymer solution than that in a hard sphere solvent. This is because the connectivity weakens the excluded-volume effect between colloids and monomers and the packing effect of the monomers.

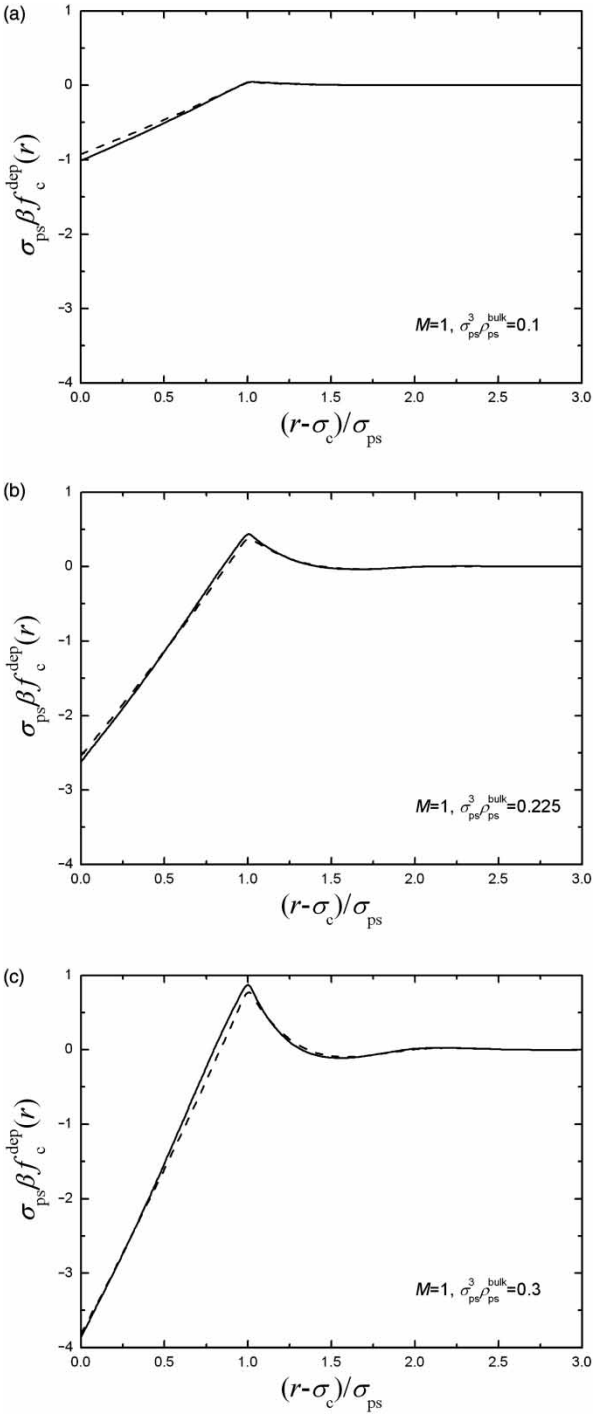

Figure 1. Depletion force between two colloidal particles in hard sphere solution; solid lines: calculated by IRDFT in this work; dashed lines: calculated by KSA method. In all calculations, $\sigma_{\mathrm{c}} = 5\sigma_{\mathrm{ps}}$.

We further compare the two versions of TPT1 and TPT2. Figure 3 shows MC and IRDFT results for the depletion force with the following three values of the

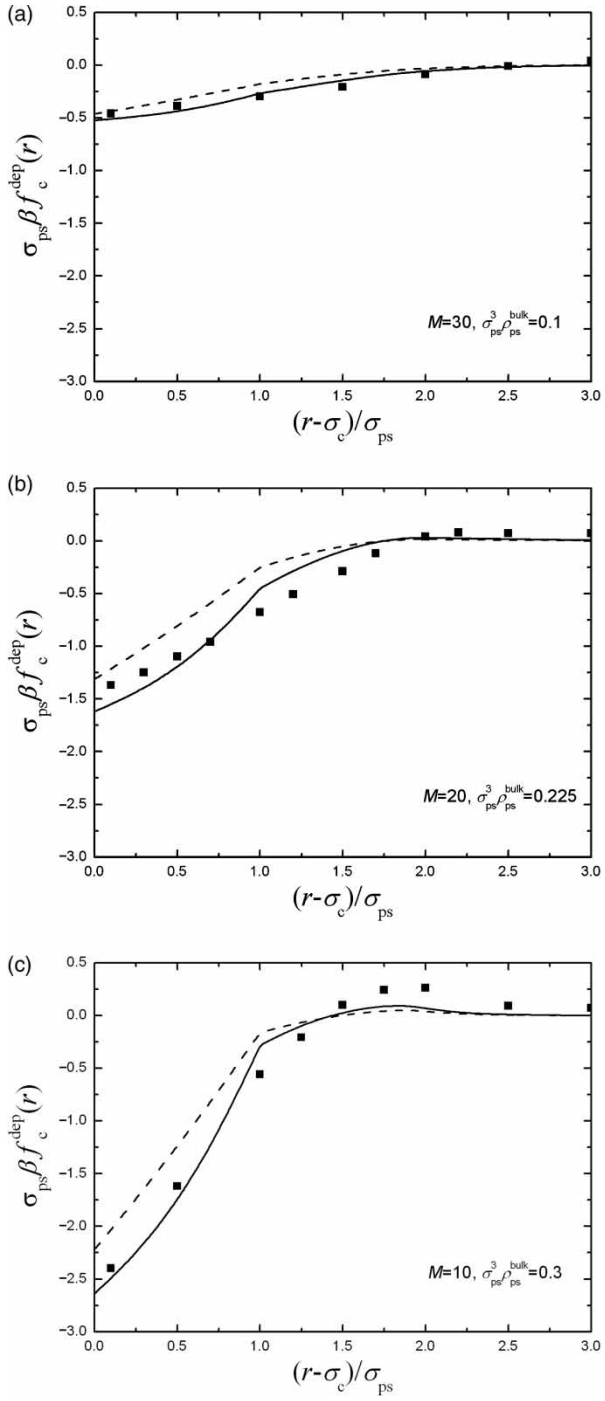

Figure 2. Depletion force between two colloidal particles in hard chain solution. Squares, MC simulation results [23]; solid lines, calculated by IRDFT in this work; dashed lines, calculated by KSA method. In all calculations, $\sigma_c = 5\sigma_{ps}$.

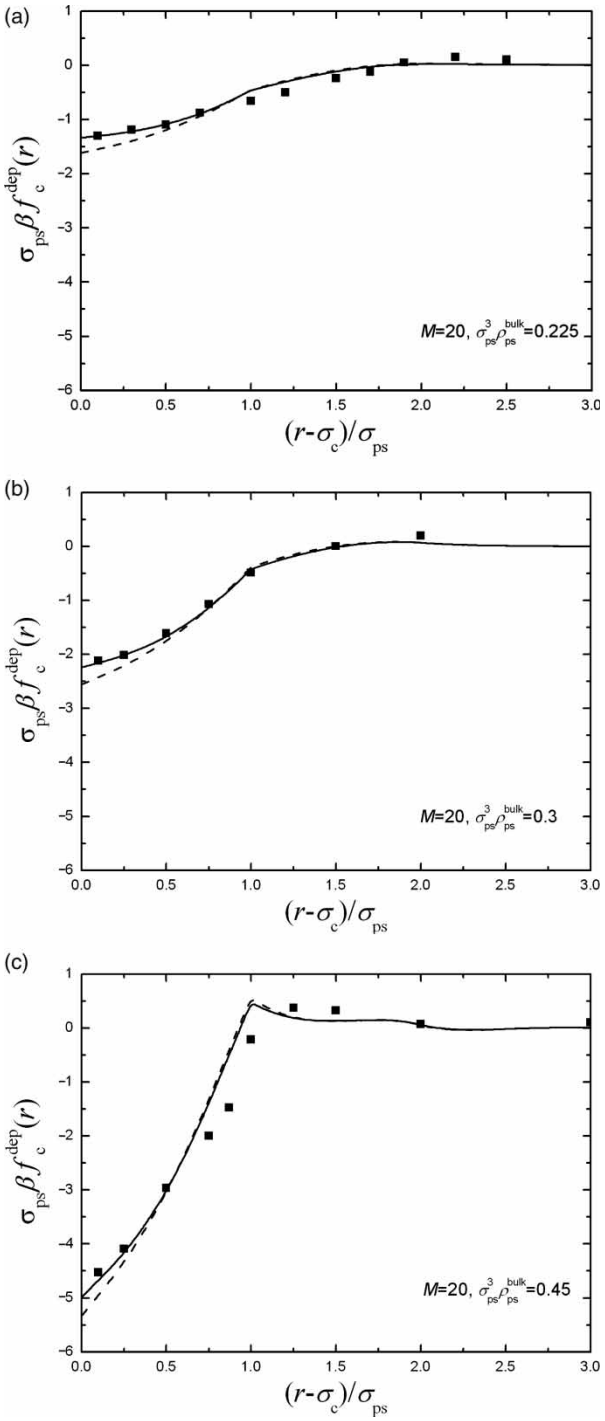

Figure 3. Depletion force between two colloidal particles in hard chain solution. Squares, MC simulation results [23]; solid lines, calculated by IRDFT and TPT2; dotted lines, calculated by IRDFT and TPT1. In all calculations, $\sigma_c = 5\sigma_{ps}$.

segment bulk density: $\sigma_{ps}^3\rho_{ps}^{bulk} = 0.225$, 0.3 and 0.45. The chain length and the colloid size are fixed at $M = 20$ and $\sigma_c = 5\sigma_{ps}$, respectively. From the figure, we can see that the results of TPT2 have a slight improvement than that of TPT1 especially in the small inter-particle distance region where the depletion force by TPT1 is too attractive. It seems that the chain connectivity described by TPT1 is less strong because only the two-body correlations are considered which may underestimate the correlations between segments which are nearest and next to nearest neighbors in a chain. TPT2 takes into account the three-body correlations which weaken the volume exclusion between colloids and polymer beads especially when two colloids are close to contact.

When we make finer comparison with the simulations, we will find that at higher polymer densities as shown in figure 3(c) where $\sigma_{ps}^3\rho_{ps}^{bulk} = 0.45$, there is a notable cusp

at $(r - \sigma_c)/\sigma_{ps} = 1$ which is higher than that in simulations. The cusp of theoretical curve reaches the maximum of the force, so the location of the maximum is at the smaller distance in comparison with simulation. The cusp is also notable in the case of colloidal particles in hard sphere solution as shown in figure 1, but it has the right height (maximum of the curve). Due to the discontinuity of the colloid–monomer potential, there is no doubt about the existence of the cusp. At high polymer densities, the packing effect is the dominant repulsive contribution to this cusp whether in polymer solution or hard sphere solution. The effect will be weakened by chain connectivity in polymer solution because the polymer stiffness obstructs the individual segments from packing into the region between two colloids. Since the TPT1 and TPT2 all take the hard sphere mixture as a reference, which is dominant at high densities, it seems that further improvement is needed to weaken the reference and to balance the competition between the excluded-volume effect and the chain connectivity.

3.2 Polymer-density dependence and chain-length dependence of the depletion force

Figures 4 and 5 show the effects of polymer density and polymer chain length on the depletion force between colloidal particles in polymer solutions. As shown in figure 4, when the polymer density increases, the depletion force is more attractive in the small inter-particle distance region. When the distance is higher, the depletion force becomes more repulsive on the contrary with the increasing polymer density. The barrier, i.e. the maximum of the curve becomes higher and moves toward the smaller distance as the polymer density increase. It seems that when the distance between two colloidal particles is less than the size of the polymer segment, the higher polymer density favorites the attractive interactions between the particles because of the excluded-volume effect similar to the case of colloid/hard sphere systems. This is not strange because the excluded-volume effect is most significant at high densities and the volume exclusion between colloids and monomers will be enhanced when two colloids are close to contact. When the distance is greater than the size of the polymer segment, although the repulsive effect is generally weak (due to the constraint of chain connectivity as analyzed before), there is still a tendency that the higher polymer density, the stronger repulsive effect indicating the more effective depletion stabilization of the particles. As for the chain-length dependence, as shown in figure 5, the barrier is almost independent of the chain length. On the other hand, when the inter-particle distance is less than the location of the maximum, except at very short distance, the longer chain length favorites the attraction between particles. The reason may lies in the stronger chain connectivity of the longer chains.

Figure 6 depicts the second virial coefficients as a function of polymer density; the figure shows the chain-length

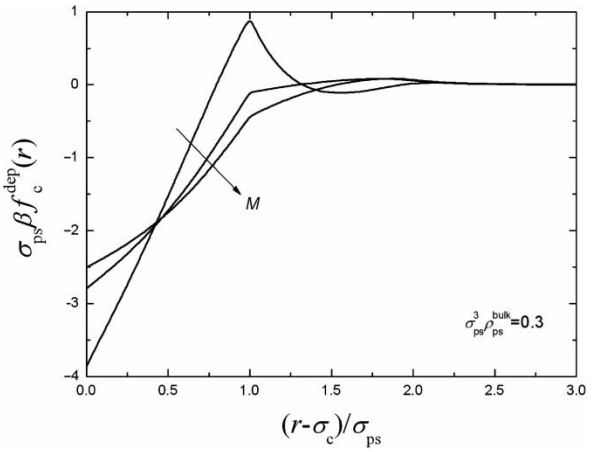

Figure 5. Chain-length dependence of depletion force between two colloidal particles in hard chain solution. $\sigma_{ps}^3\rho_{ps}^{bulk} = 0.3, \sigma_c = 5\sigma_{ps}$, $M = 1$, 5 and 50, the arrow shows the direction of greater M.

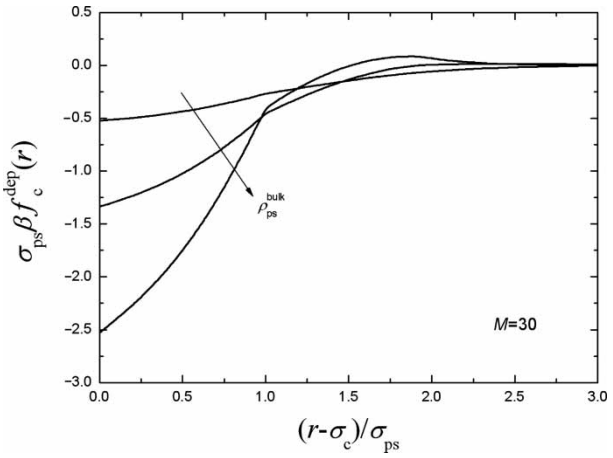

Figure 4. Polymer-density dependence of depletion force between two colloidal particles in hard chain solution. $M = 30$, $\sigma_c = 5\sigma_{ps}$, $\sigma_{ps}^3\rho_{ps}^{bulk} = 0.1, 0.2, 0.3$, the arrow shows the direction of greater ρ_{ps}.

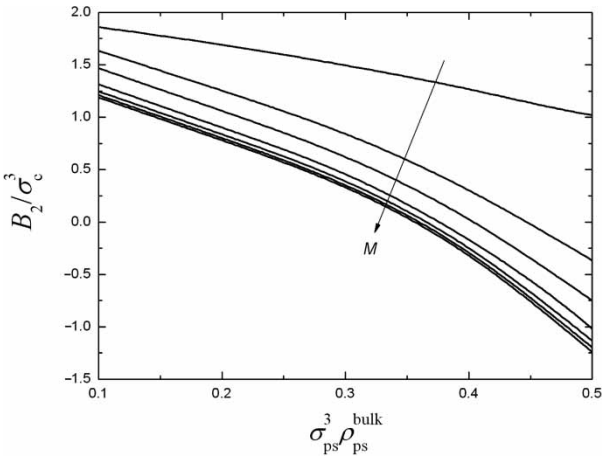

Figure 6. Chain-length dependence of the second virial coefficient as a function of polymer density. $\sigma_c = 5\sigma_{ps}$, $M = 1$, 5, 10, 20, 30, 40 and 50, the arrow shows the direction of greater M.

dependence. The effective colloidal–colloidal second virial coefficient is defined by the following relation [25]:

$$B_2 = 2\pi\int_0^\infty \mathrm{d}r r^2\{1-\exp[-\beta(V_c^{hs}(r)+V_c^{dep}(r))]\}$$
$$= \frac{2}{3}\pi\sigma_c^3 + 2\pi\int_{\sigma_c}^\infty \mathrm{d}r r^2\{1-\exp[-\beta V_c^{dep}(r)]\} \quad (18)$$

where $V_c^{hs}(r)$ is the direct intercolloidal potential, i.e. the hard sphere repulsive potential between two colloids and $V_c^{eff}(r) = V_c^{hs}(r) + V_c^{dep}(r)$ is the effective potential. As shown in the figure, generally, the second virial coefficient decreases from positive to negative as the polymer density increases indicating the stronger attractive effect in accordance with the behavior at short inter-particle distance region in figure 4. As for the chain-length dependence, the longer chain length promotes the attraction as shown by the more negative second virial coefficient conforming to that in figure 5.

3.3 Effect of the size ratio between colloid particle and polymer segment

Figure 7 depicts the effect of size ratio between colloid particle and polymer segment on the depletion force. It is shown that the higher the size ratio (the larger the colloid particle or the smaller polymer segment size), the higher the barrier indicating the more effective depletion stabilization. Inside the barrier, on the contrary, the higher size ratio induces a stronger attractive interaction between the colloidal particles. This is because the larger colloidal particles enhances the excluded-volume effect between colloids and monomers and have larger space between them to let the polymers pack into it.

Figure 8 depicts the size-ratio dependence of the second virial coefficients as a function of polymer density (a) and as a function of chain length (b). As shown in the figure, generally, the second virial coefficient decreases from positive to negative as the polymer density increases and as the chain length indicating the stronger attractive effect. On the size-ratio dependence, the higher colloidal size favorites the attraction between colloidal particles especially at higher polymer densities and longer chain length.

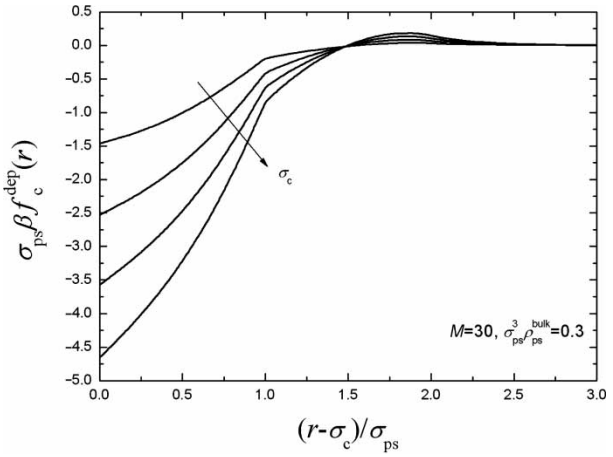

Figure 7. Effect of size ratio on depletion force between two colloidal particles in hard chain solution. $M = 30, \sigma_{ps}^3\rho_{ps}^{bulk} = 0.3$, $\sigma_c/\sigma_{ps} = 2.5$, 5, 7.5 and 10, the arrow shows the greater σ_c.

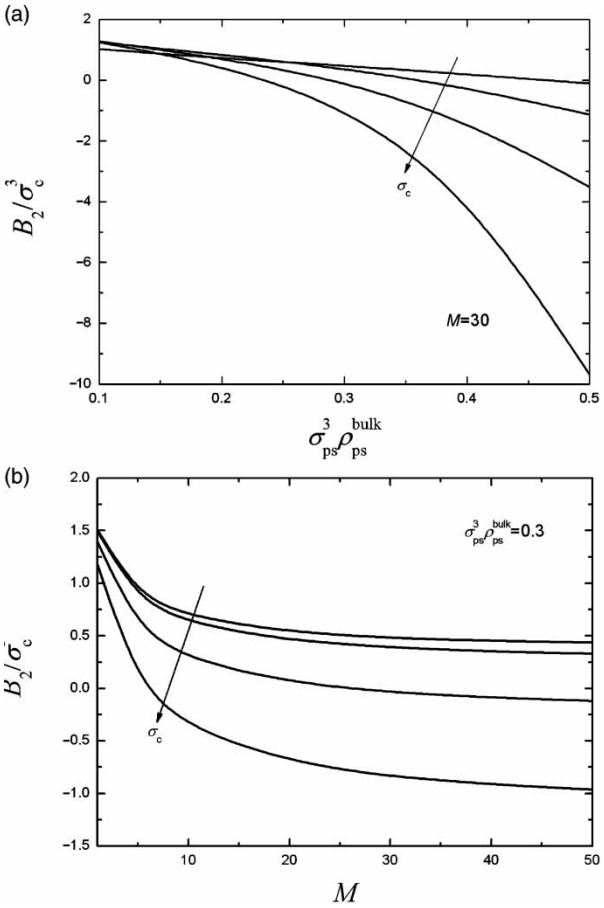

Figure 8. Size-ratio dependence of the second virial coefficient (a) as a function of polymer density, (b) as a function of chain length. $\sigma_c/\sigma_{ps} = 2.5$, 5, 7.5 and 10, the arrow shows the direction of greater σ_c.

4. Conclusions

IRDFT, modified fundamental measure theory (MFMT) and TPT1 and TPT2 are combined to study the depletion force between two colloidal particles in an athermal polymer solution. The theoretical depletion forces of hard sphere/hard sphere chain systems have been compared with simulation results over a wide range of polymer solution density and chain lengths indicating the reliability of the method used. The method captures the main characteristics of depletion interaction between colloidal particles induced by polymers. Good agreement between theory and simulation is found. Compared with BFDFT [14], which needs the two-dimensional density profile calculated from DFT, the method used in this work has much higher computational efficiency. It is more convenient to discuss the effects of the polymer density, polymer chain length and size ratio of colloid to polymer segment on the depletion force by IRDFT.

The two versions of the thermodynamic perturbation theory, TPT1 and TPT2 have been studied in detail. The results of TPT2 have shown a slight improvement than that of TPT1 especially in the small inter-particle distance region where the depletion force by TPT1 is too attractive. This gives us enlightenment that to treat the chain connectivity suitably is crucial in calculating the depletion effect in colloid/polymer systems. In TPT1, only the two-body correlations are considered which may underestimate the excluded-volume effect between segments which are nearest and next to nearest neighbors in a chain. In TPT2, because it takes into account the three-body correlations, the improvement obtained is not surprising. In our previous work [26–29], we have also adopted the next-to-nearest neighbor correlations which have shown notable improvement. However, the weighting function is based on the Tarazona's formalism [30], different from the FMT. The potential of that approach is worth to be explored.

By using the IRDFT combined with TPT1, effects of the polymer density, polymer chain length and size ratio of colloid to polymer segment on the depletion force are studied in detail.

This work can not be considered as being complete, because the prediction deteriorates when the polymer density is getting higher. The cusp occurs at $(r-\sigma_c)/\sigma_{ps}=1$ which is higher than that in simulations reminds us the hard sphere reference has played excessive role. Besides, to balance the competition between excluded-volume and chain connectivity in colloid/polymer mixture is also important. Anyway, the method presented in this work to treat the depletion interaction between hard spheres in hard sphere chain systems is useful not only because its predictions have good accuracy, but also it could be served as a basis to treat real colloids/polymer solution with complicated interactions, as well as the solution of polymer containing complex inner structure such as side chain, ring, star and the colloids with inner structures such as proteins.

Acknowledgements

This work is supported by the National Natural Science Foundation of China (Projects No. 20236010, 20490200), the Doctoral Research Foundation sponsored by the Ministry of Education of China (Project No. 20050251004), E-institute of Shanghai High Institution Grid (No. 200303) and Shanghai Municipal Education Commission of China.

A. Appendix

The excess free-energy density of the reference mixture of hard spheres has the expression

$$\Phi_{hs}=-n_0\ln(1-n_3)+\frac{n_1n_2-\mathbf{n}_{V1}\cdot\mathbf{n}_{V2}}{1-n_3}+\frac{n_2\left(n_2^2-3|\mathbf{n}_{V2}|^2\right)}{36\pi n_3^2}\left[\frac{n_3}{(1-n_3)^2}+\ln(1-n_3)\right] \quad (A1)$$

The TPT1 contribution due to the chain connectivity can be calculated by

$$\Phi_p^{TPT1}=\frac{1-M}{M}n_0^{ps}\zeta_{ps}\times\ln\left[\frac{1}{1-n_3}+\frac{n_2\sigma_{ps}\zeta}{4(1-n_3)^2}+\frac{(n_2\sigma_{ps})^2\zeta}{72(1-n_3)^3}\right] \quad (A2)$$

where $\zeta_{ps}\equiv 1-|\mathbf{n}_{V2}^{ps}|^2/(n_2^{ps})^2$, $\zeta\equiv 1-|\mathbf{n}_{V2}|^2/n_2^2$.

In FMT, the scalar and vector weighted densities are defined as

$$n_\alpha(\mathbf{r})=\sum_{i=ps,c}n_\alpha^i(\mathbf{r})\equiv\sum_{i=ps,c}\int d\mathbf{r}'\,\rho_i(\mathbf{r}')w_\alpha^i(\mathbf{r}-\mathbf{r}') \quad (A3)$$

where the subscripts $\alpha=0,1,2,3,V1,V2$ denote the index of six weight functions, in which three have the expressions

$$w_2^i(r)=\delta(\sigma_i/2-r),\quad w_3^i(r)=\Theta(\sigma_i/2-r),\quad \mathbf{w}_{V2}^i(\mathbf{r})=(\mathbf{r}/r)\delta(\sigma_i/2-r) \quad (A4)$$

The other weight functions are proportional to the above three ones,

$$w_0^i(r)=\frac{w_2^i(r)}{\pi\sigma_i^2},\quad w_1^i(r)=\frac{w_2^i(r)}{2\pi\sigma_i},\mathbf{w}_{V1}^i(\mathbf{r})=\frac{\mathbf{w}_{V2}^i(\mathbf{r})}{2\pi\sigma_i} \quad (A5)$$

References

[1] S. Asakura, F. Oosawa. On interaction between two bodies immersed in a solution of macromolecules. *J. Chem. Phys.*, **22**, 1255 (1954).
[2] T. Biben, P. Bladon, D. Frenkel. Depletion effects in binary hard-sphere fluids. *J. Phys. Condens. Matter*, **8**, 10799 (1996).
[3] R. Dickman, P. Attard, V. Simonian. Entropic forces in binary hard sphere mixtures: theory and simulation. *J. Chem. Phys.*, **107**, 205 (1997).
[4] R. Roth, R. Evans, S. Dietrich. Depletion potential in hard-sphere mixtures: theory and applications. *Phys. Rev. E*, **62**, 5360 (2000).
[5] H.H. von Grünberg, R. Klein. Density functional theory of nonuniform colloidal suspensions: 3D density distributions and depletion forces. *J. Chem. Phys.*, **110**, 5421 (1999).
[6] S. Melchionna, J.P. Hansen. Triplet depletion forces from density functional optimization. *Phys. Chem. Chem. Phys.*, **2**, 3465 (2000).
[7] D. Goulding, S. Melchionna. Accurate calculation of three-body depletion interactions. *Phys. Rev. E*, **64**, 011403 (2001).
[8] P. Attard. Pherically inhomogeneous fluids. II. Hard-sphere solute in a hard-sphere solvent. *J. Chem. Phys.*, **91**, 3083 (1989).
[9] J.P. Hansen, I.R. McDonald. *Theory of Simple Liquids*, 2nd ed., Academic Press, London (1986).
[10] W.G. McMillan, J.E. Mayer. The statistical thermodynamics of multicomponent systems. *J. Chem. Phys.*, **13**, 276 (1945).
[11] M. Dijkstra, R. van Roij, R. Evans. Phase behavior and structure of binary hard-sphere mixtures. *Phys. Rev. Lett.*, **81**, 2268 (1998); Direct simulation of the phase behavior of binary hard-sphere mixtures: test of the depletion potential description. *ibid.*, **82**, 117 (1999); Phase diagram of highly asymmetric binary hard-sphere mixtures. *Phys. Rev. E*, **59**, 5744 (1999).

[12] J.R. Henderson. Statistical mechanics of fluids at spherical structrureless walls. *Mol. Phys.*, **50**, 741 (1983).
[13] M. Oettel. Depletion force between two large spheres suspended in a bath of small spheres: Onset of the Derjaguin limit. *Phys. Rev. E*, **69**, 041404 (2004).
[14] N. Patel, S.A. Egorov. Interactions between colloidal particles in polymer solutions: A density functional theory study. *J. Chem. Phys.*, **121**, 4987 (2004).
[15] J.B. Hooper, K.S. Schweizer, R.K.T.G. Desai, P. Keblinski. Structure, surface excess and effective interactions in polymer nanocomposite melts and concentrated solutions. *J. Chem. Phys.*, **121**, 6986 (2004).
[16] M. Surve, V. Pryamitsyn, V. Ganesan. Depletion and pair interactions of proteins in polymer solutions. *J. Chem. Phys.*, **122**, 154901 (2005).
[17] S.C. Kim, C.H. Lee. Depletion interactions between colloidal particles in polymer solutions: density functional approach. *Mol. Phys.*, **104**, 1487 (2006).
[18] Y. Rosenfeld. Free-energy model for the inhomogeneous hard-sphere fluid mixture and density-functional theory of freezing. *Phys. Rev. Lett.*, **63**, 980 (1989).
[19] Y.X. Yu, J.Z. Wu. Structures of hard-sphere fluids from a modified fundamental-measure theory. *J. Chem. Phys.*, **117**, 10156 (2002).
[20] R. Roth, R. Evans, A. Lang, G. Kahl. Fundamental measure theory for hard-sphere mixtures revisited: the White Bear version. *J. Phys. Condens. Matter*, **14**, 12063 (2002).
[21] M.S. Wertheim. Thermodynamic perturbation theory of polymerization. *J. Chem. Phys.*, **87**, 7323 (1987).
[22] Y.X. Yu, J.Z. Wu. Density functional theory for inhomogeneous mixtures of polymeric fluids. *J. Chem. Phys.*, **117**, 2368 (2002).
[23] E.A. Müllar, K.E. Gubbins. Simulation of hard triatomic and tetratomic molecules A test of associating fluid theories. *Mol. Phys.*, **80**, 957 (1993).
[24] A. Striolo, C.M. Colina, K.E. Gubbins, N. Elvassore, L. Lue. The depletion attraction between pairs of colloid particles in polymer solution. *Mol. Simul.*, **30**, 437 (2004).
[25] R. Roth, R. Evans, A.A. Louis. Theory of asymmetric nonadditive binary hard-sphere mixtures. *Phys. Rev. E*, **64**, 051202 (2001).
[26] H.L. Liu, Y. Hu, J.M. Prausnitz. Equation of state for fluids containing chainlike molecules. *J. Chem. Phys.*, **104**, 396 (1996).
[27] J. Cai, H.L. Liu, Y. Hu. Density functional theory and Monte Carlo simulation of mixtures of hard sphere chains confined in a slit. *Fluid Phase Equilibria*, **194–197**, 281 (2002).
[28] S.L. Zhang, J. Cai, H.L. Liu, Y. Hu. Density functional theory of square-well chain mixtures near solid surface. *Molec. Simul.*, **30**, 143 (2004).
[29] Z.C. Ye, J. Cai, H.L. Liu, Y. Hu. Density and chain conformation profiles of square-well chains confined in a slit by density-functional theory. *J. Chem. Phys.*, **123**, 194902 (2005).
[30] P. Tarazona. Free-energy density functional for hard spheres. *Phys. Rev. A*, **31**, 2672 (1985).